ULTRASENSITIVE ULTRASOUND MICROVESSEL IMAGING FOR CHARACTERIZING BENIGN AND MALIGNANT BREAST TUMORS

Ping Gong[*], **Pengfei Song**[*], **Chengwu Huang**[*], **U-Wai Lok**[*], **Shanshan Tang**[*], **Yue Yu**[†], **Duane D. Meixner**[*], **Kathryn J. Ruddy**[‡], **Karthik Ghosh**[§], **Robert T. Fazzio**[*], **Wenwu Ling**[*,¶], **Shigao Chen**[*]

[*]Department of Radiology, Mayo Clinic, Rochester, Minnesota, USA

[†]Department of Health Sciences Research, Mayo Clinic, Rochester, Minnesota, USA

[‡]Department of Oncology, Mayo Clinic, Rochester, Minnesota, USA

[§]Department of General Internal Medicine, Mayo Clinic, Rochester, Minnesota, USA

[¶]Department of Ultrasound, West China Hospital of Sichuan University, Chengdu, Sichuan, China

Abstract

Tumor angiogenesis plays an important role during breast tumor growth. However, conventional Doppler has limited sensitivity to detect small blood vessels, resulting in a large overlap of Doppler features between benign and malignant tumors. An ultrasensitive ultrasound microvessel imaging (UMI) technique was recently developed. To evaluate the performance of UMI, we studied 44 patients with 51 breast masses. Tumor pathology served as the gold standard: 28 malignancies and 23 benignities. UMI provided a significant improvement in depicting smaller vessels compared with conventional Doppler. The microvessel morphologies observed on UMI were associated with tumor benign/malignant classification. The diagnostic accuracy of correct Breast Imaging Reporting and Data System (BI-RADS) classification rate (BI-RADS 4a: test positive; BI-RADS 3: test negative) as a fraction of total mass population was improved by 16% after combining conventional ultrasound with UMI compared with using conventional ultrasound alone. This improvement indicates the potential of UMI in reducing unnecessary benign biopsies and avoiding missed malignant biopsies.

Keywords

Microvessel imaging; Ultrafast ultrasound imaging; Tumor angiogenesis; Breast tumor differentiation; Doppler sensitivity

INTRODUCTION

Breast cancer is the most common neoplasm and the most frequent cause of death in women between 35 and 55 y of age (Nothacker et al. 2009; Pyakurel et al. 2014). Ultrasonography

Address correspondence to: Wenwu Ling, Department of Ultrasound, West China Hospital of Sichuan University, Chengdu, 610041, Sichuan, China. hxlww@outlook.com.

(US) is a common adjunct to mammography for breast cancer screening because it is cost effective, widely available and safe (Smith et al. 2003). Tumor features on gray-scale US (*e.g.*, echotexture, orientation, margin analysis, posterior acoustic features) provide diagnostic information for tumor classification, as summarized in the Breast Imaging Reporting and Data System (BI-RADS) (Smith et al. 2003; D'Orsi 2013). Some occult breast cancers are detected by US but not mammography, particularly in women with dense breasts (Gordon & Goldenberg 1995; Kolb et al. 1998; Berg et al. 2008). Combined screening with ultrasound and mammography has been found to improve diagnostic sensitivity compared with mammography alone (Berg et al. 2008). However, this combined approach also increases the number of false positives caused by the low specificity of conventional US, resulting in a large number of unnecessary benign biopsies (Berg et al. 2008; Nothacker et al. 2009). To increase the diagnostic accuracy of US, studies using new and innovative ultrasound diagnostic techniques have been carried out for early-stage tumor detection and classification (Du et al. 2012; Liu et al. 2014; Lee et al. 2017). Among these studies, characterization of tumor vessel morphology has shown clinical promise (Weind et al. 1998; Uzzan et al. 2004; Chang et al. 2012; Pyakurel et al. 2014; Ma et al. 2015; Yongfeng et al. 2016). In contrast to normal tissue and benign tumors, malignant tumors typically present a vessel pattern with chaotic distribution, irregular branches and penetrating peripheral vasculature (Chang et al. 2012). Ultrasound Doppler techniques are often used to investigate tumor angiogenesis in breast cancers (Lee et al. 2002; Cha et al. 2007; Gokalp et al. 2009). However, the clinical reliability of conventional Doppler is undermined by limited vessel detection sensitivity (Ma et al. 2015). This is because conventional Doppler technologies are generally based on line-by-line focused-beam scanning (Ma et al. 2015; Park et al. 2016). The low frame rate limits the number of image frames available for Doppler processing and, thus, limits the Doppler sensitivity of vessel detection (Mace et al. 2013). The performance of conventional Doppler is also hindered by tissue clutter caused by tissue motion because the tissue motions produce similar Doppler signals as the low-velocity flow components. A temporal-domain wall filter is typically applied in conventional Doppler to remove clutter: echoes with low movement speed are assumed to be tissues and rejected. Therefore, vessels containing blood flows with speed lower than the tissue rejection threshold, so-called microvessels, are filtered out and cannot be detected (Schroeder et al. 2003; Park et al. 2016). Unfortunately, these microvessels usually contain valuable tumor angioneogenesis information, such as tortuous vessel course, disturbed dichotomous branching and decreasing vessel caliber, which have been closely correlated with malignant tumor growth (Schroeder et al. 2003). Because of the loss of tumor microvessel information, the vessel features detected in benign and malignant tumors often exhibit significant overlaps in conventional Doppler (Park and Seo 2018). Consequently, novel Doppler technologies with significantly improved vessel detection sensitivity are important to facilitate more accurate breast tumor classification. Recently, the emergence of ultrafast ultrasound imaging offers new opportunities for enhanced Doppler sensitivities by significantly increasing the number of frames available for Doppler imaging (Montaldo et al. 2009). An ultrasensitive ultrasound microvessel imaging (UMI) technique was proposed to provide advanced vessel sensitivity and superior tissue rejection without using ultrasound contrast agents (Song et al. 2017a, 2017b, 2018). The microvessels detected in UMI may provide new possibilities of breast tumor characterization with US.

This study aimed to investigate the feasibility of UMI to assess the breast tumor microvessel distribution. This study also evaluated the combination of UMI and conventional US in differentiating benign from malignant masses.

METHODS

An institutional review board-approved prospective study was carried out to investigate the feasibility of using UMI to differentiate breast masses based on mass vascularity. Written informed consent was obtained at the time of enrollment of each participant.

Study population

Between March 2016 and June 2018, 44 breast patients scheduled for clinically indicated biopsy were enrolled, including 1 male (age: 83 y) and 43 females (mean age: 48 y, range: 24–79 y). Thirty-seven patients had a solitary mass, and 7 patients had two masses (51 masses in total). The maximum diameter of studied masses ranged from 0.7–5.0 cm (mean ± standard deviation [SD]: 2.0 ± 1.1 cm). Histopathological results were available for all patients from core needle biopsy and served as the gold standard, which revealed 23 benign and 28 malignant masses (as listed in Table 1). All 44 patients completed our research protocol examination on the day of biopsy or at least 14 d after the biopsy, before any treatment.

Study protocol: Conventional US and UMI

In our study protocol, a conventional US scan was first conducted by one of two experienced sonographers, depending on their availability (one with >28 y and the other with >10 y of experience in breast US). Conventional US exams were conducted using the General Electric LOGIQ E9 and a 9 L linear array probe (GE Healthcare, Wauwatosa, WI, USA). After the target mass was localized, gray-scale B-mode imaging and conventional Doppler were conducted in both long-axis and short-axis views (three repeated acquisitions in each view, six acquisitions in total). The parameter settings of B-mode and conventional Doppler were adjusted by the sonographer until the image quality was visually optimized for each tumor studied. Afterward, UMI was performed in the same imaging planes (two views, six acquisitions in total) using a Verasonics Vantage system (Verasonics Inc., Kirkland, WA, USA) equipped with the same 9 L probe. The study protocol (conventional US + UMI scans) for each participant was completed within 30 min. The UMI data obtained were processed using a recently developed clutter filtering technique (Song et al. 2017a). The role of the clutter filter applied in UMI is equivalent to the temporal-domain wall filter that is typically applied in conventional Doppler imaging. Instead of using the temporal information alone to reject tissue as in the wall filter, the advanced clutter filter leverages both temporal and spatial information to selectively reject tissue signals or noise and extract microvessel signals. The clutter filter required several minutes of computation time and, therefore, was applied during offline processing. Accelerated clutter filtering as described in Song et al. (2017b) may be implemented in the future for real-time UMI application. Power Doppler signals of microvessels overlaid on B-mode images were used for the analysis described next.

Tumor microvessel analysis

The quantitative/qualitative parameters derived to characterize benign and malignant breast masses in UMI images were as follows:

Vessel density.—Vessel density (VD) is defined as the number of vessel pixels divided by the overall number of pixels of the mass (Weind et al. 1998; Chang et al. 2012), as illustrated in Figure 1a. VD was also used as a performance metric to compare the vessel detection sensitivity of conventional Doppler and UMI.

Periphery-to-center vessel density ratio.—The mass region was evenly divided (by area) into peripheral and central regions. The central region was generated by shrinking the mass boundary inward until the area inside the new boundary (*i.e.*, central region) was half of the entire tumor area. The area between the new boundary and the original boundary is defined as the peripheral region, as illustrated in Figure 1b. The periphery-to-center vessel density ratio (VDR) was calculated as the ratio of peripheral VD to central VD (Liu et al. 2014). Therefore, VDR describes the vessel distributions inside a mass at the periphery (VDR>1), center (VDR<1) or both (VDR $\approx$ 1).

Microvessel morphology.—Another UMI evaluation criterion was the microvessel morphologic difference inside (*i.e.*, intratumor) and outside (*i.e.*, peritumor) the tumor boundary. A radiologist (with > 10 y of experience in breast US), blinded to pathology results, first assigned a BI-RADS score to each breast mass using conventional US (*i.e.*, B-mode and conventional Doppler). In current clinical practice, tumors in BI-RADS categories ≥ 4a are considered as test positive and would require biopsy; tumors in BI-RADS categories ≤ 3 are considered test negative and would not need biopsy. Then the same radiologist adjusted the BI-RADS score based on the microvessel morphology obtained from UMI, according to the criteria specified in Table 2. The original BI-RADS score was downgraded by up to two categories (−1, −2), upgraded by up to two categories (+1, +2) or not changed (0) based on the microvessel features obtained in UMI. Representative UMI images are discussed in the Results.

Statistical analysis

Statistical analyses were performed with MedCalc (Software Version 18.6, Ostend, Belgium). An averaged VD was calculated for each breast mass (two views, three acquisitions at each view) to compare the vessel detection sensitivity of conventional Doppler and UMI. A higher VD indicates better detection sensitivity. A two-tailed Wilcoxon rank-sum test ($p < 0.05$) was used for comparison. The VD and VDR acquired in UMI were also compared between benign and malignant tumors using a two-tailed Mann–Whitney rank-sum test ($p < 0.05$). Moreover, tumor BI-RADs categories before and after regrading were correlated with tumor pathologies (biopsy-proven malignancy: true positive, biopsy-proven benignity: true negative) to calculate the diagnostic sensitivity, specificity, positive predictive value (PPV), negative predictive value (NPV) and accuracy (ACC).

RESULTS

Improved vessel detection sensitivity of UMI over conventional Doppler

VD was used as the performance metric to compare the vessel detection sensitivity of conventional Doppler and UMI (a higher VD indicates better detection sensitivity). UMI provided significantly improved vessel detection sensitivity compared with conventional Doppler using the two-tailed Wilcoxon rank-sum test ($p < 0.05$). Figure 2 illustrates two representative cases: (a) and (b) are conventional Doppler and UMI images of a 43-y-old woman with a fibroadenoma mass; (c) and (d) conventional Doppler and UMI images of a 40-y-old woman with an invasive ductal carcinoma mass. In both cases, small blood vessels that were undetectable under conventional Doppler could be clearly visualized in UMI. The UMI of fibroadenoma exhibits relatively regular or linear vessel distribution with intratumor vessels isolated from peritumor vessels. The UMI of fibroadenoma also exhibits a continuous blood vessel running along the mass boundary, which is not presented in conventional Doppler. On the other hand, the UMI of carcinoma has relatively chaotic vessel morphologies with the intra- and peritumor vessel networks closely connected. The significantly improved vessel sensitivity of UMI allowed better evaluation of breast tumor vascular morphology and distribution, which were difficult to see with conventional Doppler.

VD and VDR in benign and malignant breast masses

Figure 3 (a, b) summarize the VD and VDR measurements in the studied masses. With UMI, the VDs of benign and malignant tumors were $13.1 \pm 11.3\%$ and $13.7 \pm 10.6\%$ (mean ± SD), respectively. The mean VDRs of benign and malignant tumors were 2.74 ± 3.03 and 3.79 ± 5.97, respectively. No significant differences in VD or VDR between these two groups were detected ($p > 0.05$).

Microvessel morphology differences in benign and malignant breast masses

The intra- and peritumor microvessel morphologies obtained with UMI were then used for tumor regrading according to Table 2. Figure 4 provides some representative UMI images for different types of breast masses. The original BI-RAD scores based on conventional US and the BI-RADS scores regraded with UMI are both provided in the subtitle of each mass image. Fibroadenomas (Fig. 4a–c) are hypervascular at both the mass center and periphery. The vessel morphologies agree well with the descriptions as summarized in Table 2 for benign masses— regular or linear vessel distribution with intratumor vessels isolated from peritumor vessels. Another major vessel feature for fibroadenoma is the presence of a continuous blood vessel running along the mass boundary. This feature was observed in UMI rather than conventional Doppler thanks to the high vessel detection sensitivity of UMI. For fibrocystic changes (Fig. 4d–f), conventional Doppler and UMI revealed similar vessel morphologies: avascular/hypovascular at both mass center and periphery. The vessel density differences between fibroadenoma and fibrocystic changes explain the wide range of VD distribution in benign masses (Fig. 3a). For carcinomas (Fig. 4g–i), the VD/VDR in the tumors varies from case to case, which may be related to different tumor stages. The vessel morphologies follow a tortuous course and have a chaotic distribution with irregular

branches as described in Table 2. The intra- and peritumor microvessel networks were also closely connected with penetrating vessels extending outside of the tumor.

In Figure 5 are the scatterplots for (a) original BI-RADs scores based on conventional US/Doppler and (b) regraded BI-RADS scores after combining conventional US with UMI. After regrading, seven false-positive benign tumors were downgraded from BI-RADS categories 4a/4b to 3, which would avoid biopsy. Five malignant tumors were upgraded to BI-RADS category 5. One false-negative malignant tumor originally in BI-RADS category 3 was upgraded to 4b, which does require biopsy. Table 3 summarizes the statistical analysis before and after regrading. Compared with conventional US alone, the combination of conventional US and UMI led to significant improvements (one-tailed McNemar test, $p <$ 0.05) in diagnostic sensitivity (+4%), specificity (+30%), PPV (+11%), NPV (+20%) and ACC (+16%).

DISCUSSION

This study investigated the feasibility of combining UMI and conventional US to facilitate more accurate differentiation of benign and malignant breast tumors. In comparison to conventional Doppler, UMI provided significantly improved vessel detection sensitivity. This improvement can be attributed to different UMI imaging principles. Instead of line-by-line scanning as in conventional Doppler, UMI is based on ultrafast plane wave imaging, by which 500–4000 Doppler temporal ensembles can be accumulated within 1 s (Montaldo et al. 2009). This leads to at least 10 times more ultrasound frames for blood flow detection than conventional Doppler (which typically uses only 16 frames). The larger number of frames leads to higher flow sensitivity, allowing smaller vessels that are undiscernible in conventional Doppler to be detected. In addition, an advanced clutter filter leverages both spatial and temporal information to robustly separate blood signal from tissue clutters and noise (Song et al. 2017a), further improving UMI's performance in vessel detection. The overall enhancement allows imaging of breast tumor vascularity in greater detail without the need to use contrast microbubbles.

VD and VDR have been used in Doppler imaging to assess breast tumor angiogenesis (Weind et al. 1998; Chang et al. 2012; Liu et al. 2014). However, no consensus on VD/VDR tumor classification cutoffs has been reached because of the considerable overlaps of these parameters between benign and malignant tumors (Burns et al. 2000; Gokalp et al. 2009; Du et al. 2012). In this study, we did not observe significant differences in VD and VDR between benign and malignant masses. The benign masses can be both hypervascular (*e.g.*, fibroadenoma) and hypovascular/avascular (*e.g.*, fibrocystic change). The VD in malignant tumors varies from case to case, which may be related to tumor stage. Early-stage malignant tumors (*e.g.*, grade I or II) typically have rich vascularity because of enhanced angiogenesis (Ma et al. 2015). In contrast, at later stages (*e.g.*, grade III), the rapid tumor growth may lead to necrosis and, thus, hypovascularity at the tumor center (Metz et al. 2003; Du et al. 2012). Moreover, the boundaries of malignant tumors are usually speculated and not well defined, which makes it difficult to accurately calculate VD or VDR inside a malignant tumor. In addition, the central region selected as half of the entire tumor area to determine VDR was also relatively arbitrary. Future studies with larger samples may be needed to investigate the

optimal partition of tumor central and peripheral areas to determine if performance of VDR can be improved. These challenges may have led to the low performance of VD and VDR. Another drawback of VD and VDR quantification is that these parameters only assess the intratumor vascularity but ignore the surrounding vascular features, which also contain important diagnostic information (Chang et al. 2012). In this study, VD and VDR were only evaluated in two orthogonal planes so that the measurements were not comprehensive and may vary with the selected scanning planes. In the future, the UMI technique can be extended to 3-D imaging to provide a more thorough microvessel evaluation (Chang et al. 2012).

In contrast to VD and VDR, the adjustment of BI-RADS scores through qualitative assessment of UMI images did not require accurate determination of tumor boundary: only the microvessel morphologies as summarized in Table 2 were used. Therefore, the approach is less sensitive (compared with VD and VDR) to determination of tumor boundary, which may be one of the reasons that this approach had better diagnostic performance than VD and VDR. The addition of vascular features from UMI offered improved accuracy in differentiating benign from malignant tumors compared with BI-RADS using conventional US alone. The accuracy improvement exhibited a good association between the microvessel morphologic characteristics and breast tumor classifications. The high vessel detection sensitivity offered by UMI allows more detailed vascular evaluation than conventional Doppler, potentially facilitating more accurate breast cancer diagnosis with ultrasound. In future studies, vessel morphology-related tortuosity may be quantitatively measured with parameters such as distance metric and sum of angle metric as described in Bullitt et al. (2003). Note that both B-mode and conventional Doppler images were used to assign the original BI-RADS score for each tumor. However, the weighting of conventional Doppler images was very low in original BI-RADS grading. When UMI images were used to adjust BI-RADS scores, the contribution of conventional Doppler was further reduced to minimal, because UMI had higher sensitivity and thus UMI images already included all vessels detected by conventional Doppler. Therefore, our study is essentially a comparison between B-mode + Doppler and B-mode + UMI. Nevertheless, we acknowledge that our study includes three modalities (B-mode, conventional Doppler and UMI) and thus is not a straight head-to-head comparison with conventional two-modality BI-RADS (B-mode and conventional Doppler), which is a limitation. On the other hand, the goal is to improve the diagnostic accuracy of ultrasound, instead of replacing conventional Doppler with UMI. Therefore, the use of one more modality can be justified if the combination leads to improved performance. Another limitation of this study is that we did not systematically compare the performance of UMI with that of other existing microvessel technologies (*e.g.*, Superb Microvessel Imaging, Toshiba Medical Systems Corp., Tokyo, Japan). Future study may be needed in this area. Furthermore, we have not investigated operator dependency, which is a limitation of this study. Patients were scanned by one of two experienced sonographers (one with >28 y and the other with >10 y of experience). For each patient, the same sonographer acquired both conventional Doppler images and UMI images in standard long-axis and short-axis views, which may help reduce variation caused by selection of imaging planes for fair comparison between conventional Doppler and UMI images. UMI requires a high-frame-rate plane wave imaging system and, thus, is not available on low-

frame-rate line-by-line ultrasound scanners. As clinical ultrasound systems with plane wave imaging capability are becoming more common, we expect that UMI will be more accessible in the future.

Another limitation of our study is the small number of patients and limited types of tumors included in this study. A prospective clinical study with a larger sample size would be beneficial. In addition, only patients who were scheduled for clinically indicated breast tumor biopsy were recruited in this pilot study (to obtain pathology results). Therefore, patients enrolled in this study had mainly BI-RADS 4 and 5 category tumors, leading to more malignant cases in the studied population. A more comprehensive patient pool with wider BI-RADS category distribution may be beneficial in future studies to explore the additional clinical values of UMI. In this study, the radiologist had no previous experience in using UMI for regrading because UMI is a newly developed technology and this is the first study applying UMI in breast tumor classification. Considering the small sample size, we did not provide additional UMI images to train the radiologist before he adjusted the BI-RADS categories with UMI. The diagnostic accuracy may be further improved with more experience.

CONCLUSIONS

Ultrasensitive UMI provided significantly improved vessel detection sensitivity compared with conventional Doppler. The combined use of UMI and conventional US improved diagnostic accuracy in tumor differentiation compared with conventional US alone. The microvessel information provided by UMI may add clinical value to supplemental US screening adjunct to mammography in reducing unnecessary and missed biopsies.

Acknowledgments—

REFERENCES

Berg WA, Blume JD, Cormack JB, Mendelson EB, Lehrer D, Bohm-Velez M, Pisano ED, Jong RA, Evans WP, Morton MJJJ. Combined screening with ultrasound and mammography vs mammography alone in women at elevated risk of breast cancer. JAMA 2008;299:2151–2163. [PubMed: 18477782]

Bullitt E, Gerig G, Pizer SM, Lin W, Aylward SR. Measuring tortuosity of the intracerebral vasculature from MRA images. IEEE Trans Med Imaging 2003;22:1163–1171. [PubMed: 12956271]

Burns PN, Wilson SR, Simpson DH. Pulse inversion imaging of liver blood flow: Improved method for characterizing focal masses with microbubble contrast. Invest Radiol 2000;35:58–71. [PubMed: 10639037]

Cha JH, Moon WK, Cho N, Kim SM, Park SH, Han B-K, et al. Characterization of benign and malignant solid breast masses: Comparison of conventional US and tissue harmonic imaging. Radiology 2007;242:63–69. [PubMed: 17090709]

Chang YC, Huang YH, Huang CS, Chang RF. Vascular morphology and tortuosity analysis of breast tumor inside and outside contour by 3-D power Doppler ultrasound. Ultrasound Med Biol 2012;38:1859–1869. [PubMed: 22975041]

D'Orsi CJ. ACR BI-RADS atlas: Breast Imaging Reporting and Data System. Reston, VA: American College of Radiology; 2013.

Du J, Wang L, Wan CF, Hua J, Fang H, Chen J, Li FH. Differentiating benign from malignant solid breast lesions: Combined utility of conventional ultrasound and contrast-enhanced ultrasound in comparison with magnetic resonance imaging. Eur J Radiol 2012;81: 3890–3899. [PubMed: 23062280]

Gokalp G, Topal U, Kizilkaya E. Power Doppler sonography: Anything to add to BI-RADS US in solid breast masses? Eur J Radiol 2009;70:77–85. [PubMed: 18243623]

Gordon PB, Goldenberg SLJC. Malignant breast masses detected only by ultrasound. A retrospective review. Cancer 1995;76:626–630. [PubMed: 8625156]

Kolb TM, Lichy J, Newhouse JHJR. Occult cancer in women with dense breasts: Detection with screening US—Diagnostic yield and tumor characteristics. Radiology 1998;207:191–199. [PubMed: 9530316]

Lee SW, Choi HY, Baek SY, Lim SM. Role of color and power Doppler imaging in differentiating between malignant and benign solid breast masses. J Clin Ultrasound 2002;30:459–464. [PubMed: 12242733]

Lee SH, Chung J, Choi HY, Choi SH, Ryu EB, Ko KH, Koo R, Park JS, Yi A, Youk JH, Son EJ, Chu AJ, Chang JM, Cho N, Jang MJ, Kook SH, Cha ES, Moon WK. Evaluation of screening US—detected breast masses by combined use of elastography and color Doppler US with B-mode US in women with dense breasts: A multicenter prospective study. Radiology 2017;285:660–669. [PubMed: 28640693]

Liu H, Jiang Y, Dai Q, Zhu Q, Wang L, Lu J. Peripheral enhancement of breast cancers on contrast-enhanced ultrasound: Correlation with microvessel density and vascular endothelial growth factor expression. Ultrasound Med Biol 2014;40:293–299. [PubMed: 24315392]

Ma Y, Li G, Li J, Ren WD. The diagnostic value of superb microvascular imaging (SMI) in detecting blood flow signals of breast lesions: A preliminary study comparing SMI to color Doppler flow imaging. Medicine 2015;94(36):e1502. [PubMed: 26356718]

Mace E, Montaldo G, Osmanski BF, Cohen I, Fink M, Tanter M. Functional ultrasound imaging of the brain: Theory and basic principles. IEEE Trans Ultrason Ferroelectr Freq Control 2013;60:492–506. [PubMed: 23475916]

Metz S, Daldrup-Link HE, Richter T, Räth C, Ebert W, Settles M, Rummeny EJ, Link TM, Piert M. Detection and quantification of breast tumor necrosis with MR imaging: Value of the necrosis-avid contrast agent gadophrin-3. Acad Radiol 2003;10:484–90. [PubMed: 12755535]

Montaldo G, Tanter M, Bercoff J, Benech N, Fink M. Coherent plane-wave compounding for very high frame rate ultrasonography and transient elastography. IEEE Trans Ultrason Ferroelectr Freq Control 2009;56:489. [PubMed: 19411209]

Nothacker M, Duda V, Hahn M, Warm M, Degenhardt F, Madjar H, Weinbrenner S, Albert US. Early detection of breast cancer: Benefits and risks of supplemental breast ultrasound in asymptomatic women with mammographically dense breast tissue. A systematic review. BMC Cancer 2009;9:335. [PubMed: 19765317]

Park AY, Seo BK. Up-to-date Doppler techniques for breast tumor vascularity: Superb microvascular imaging and contrast-enhanced ultrasound. Ultrasonography 2018;37:98–106. [PubMed: 29025210]

Park AY, Seo BK, Cha SH, Yeom SK, Lee SW, Chung HH. An innovative ultrasound technique for evaluation of tumor vascularity in breast cancers: Superb micro-vascular imaging. J Breast Cancer 2016;19:210–213. [PubMed: 27382399]

Pyakurel D, Karki S, Agrawal C. A study on microvascular density in breast carcinoma. J Pathol Nepal 2014;4:570–575.

Schroeder R-J, Bostanjoglo M, Rademaker J, Maeurer J, Felix R. Role of power Doppler techniques and ultrasound contrast enhancement in the differential diagnosis of focal breast lesions. Eur J Radiol 2003;13:68–79.

Smith RA, Saslow D, Sawyer KA, Burke W, Costanza ME, Evans WP, Foster RS, Hendrick E, Eyre HJ, Sener S. American Cancer Society guidelines for breast cancer screening: Update 2003. CA Cancer J Clin 2003;53:141–169. [PubMed: 12809408]

Song P, Manduca A, Trzasko JD, Chen S. Ultrasound small vessel imaging with block-wise adaptive local clutter filtering. IEEE Trans Med Imaging 2017;36:251–262. [PubMed: 27608455]

Song P, Trzasko JD, Manduca A, Qiang B, Kadirvel R, Kallmes DF, et al. Accelerated singular value-based ultrasound blood flow clutter filtering with randomized singular value decomposition and randomized spatial downsampling. IEEE Trans Ultrason Ferroelectr Freq Control 2017;64:706–716. [PubMed: 28186887]

Song P, Trzasko JD, Manduca A, Huang R, Kadirvel R, Kallmes DF, Chen S. Improved super-resolution ultrasound microvessel imaging with spatiotemporal nonlocal means filtering and bipartite graph-based microbubble tracking. IEEE Trans Ultrason Ferroelectr Freq Control 2018;65:149–167. [PubMed: 29389649]

Uzzan B, Nicolas P, Cucherat M, Perret GY. Microvessel density as a prognostic factor in women with breast cancer: A systematic review of the literature and meta-analysis. Cancer Res 2004;64:2941–2955. [PubMed: 15126324]

Weind KL, Maier CF, Rutt BK, Moussa M. Invasive carcinomas and fibroadenomas of the breast: Comparison of microvessel distributions—Implications for imaging modalities. Radiology 1998;208:477–483. [PubMed: 9680579]

Yongfeng Z, Ping Z, Wengang L, Yang S, Shuangming T. Application of a novel microvascular imaging technique in breast lesion evaluation. Ultrasound Med Biol 2016;42:2097–2105. [PubMed: 27321174]

$$(a)$$
$$VD\% = \frac{\text{vessel pixels}}{\text{overall tumor pixels}} \times 100\%$$
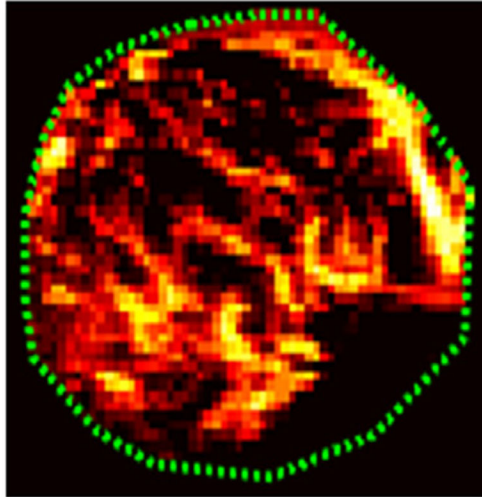
$$(b)$$
$$VDR = \frac{\text{peripheral VD}}{\text{center VD}}$$
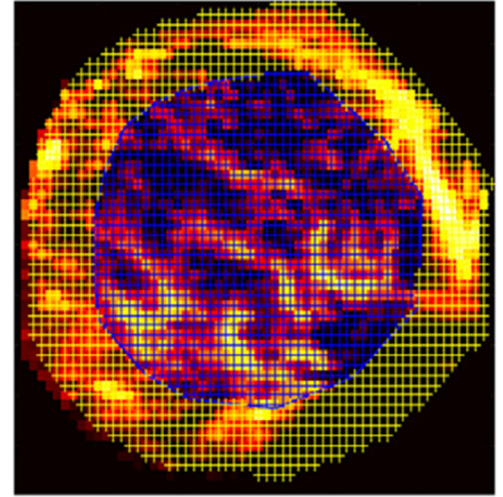
Fig. 1.
Vessel density (VD) and vessel density ratio (VDR) calculation using ultrasensitive ultrasound microvessel imaging (UMI). (a) VD calculation using an example UMI image of a 27-y-old woman with a fibroadenoma mass. The *green dashed lines* indicate the mass boundary. (b) VDR calculation example using the same mass. The *blue*-shaded area indicates the center region, and the *yellow*-shaded area indicates the periphery.
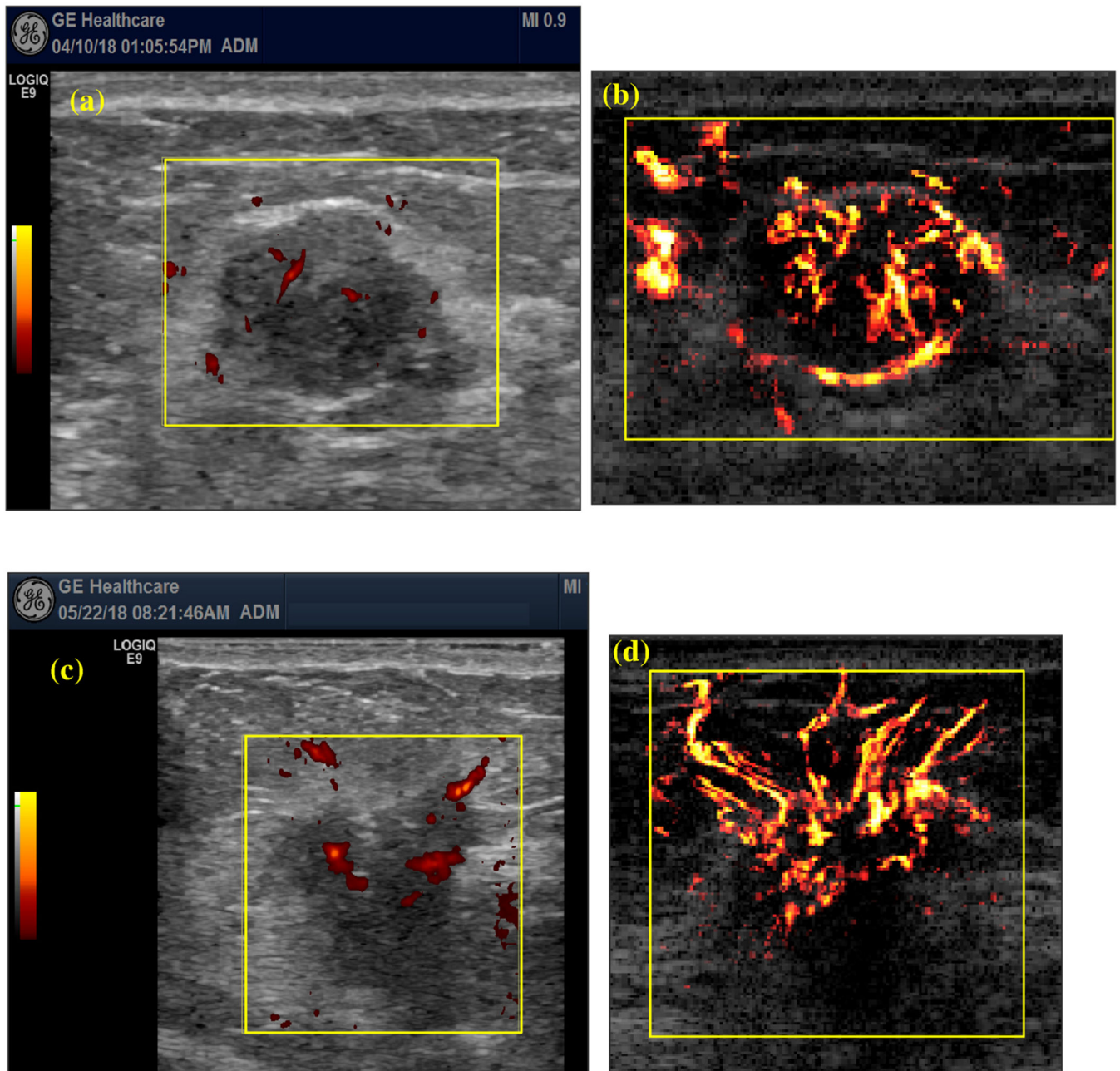
Fig. 2.
Comparison of vessel detection sensitivity between conventional Doppler and ultrasensitive ultrasound microvessel imaging (UMI). (a) Conventional Doppler and (b) UMI images of a 43-y-old woman with a fibroadenoma mass. Maximum mass diameter: 2.0 cm. (c) Conventional Doppler and (d) UMI images of a 40-y-old woman. Nottingham grade I (of III) invasive ductal. Maximum mass diameter: 1.9 cm.
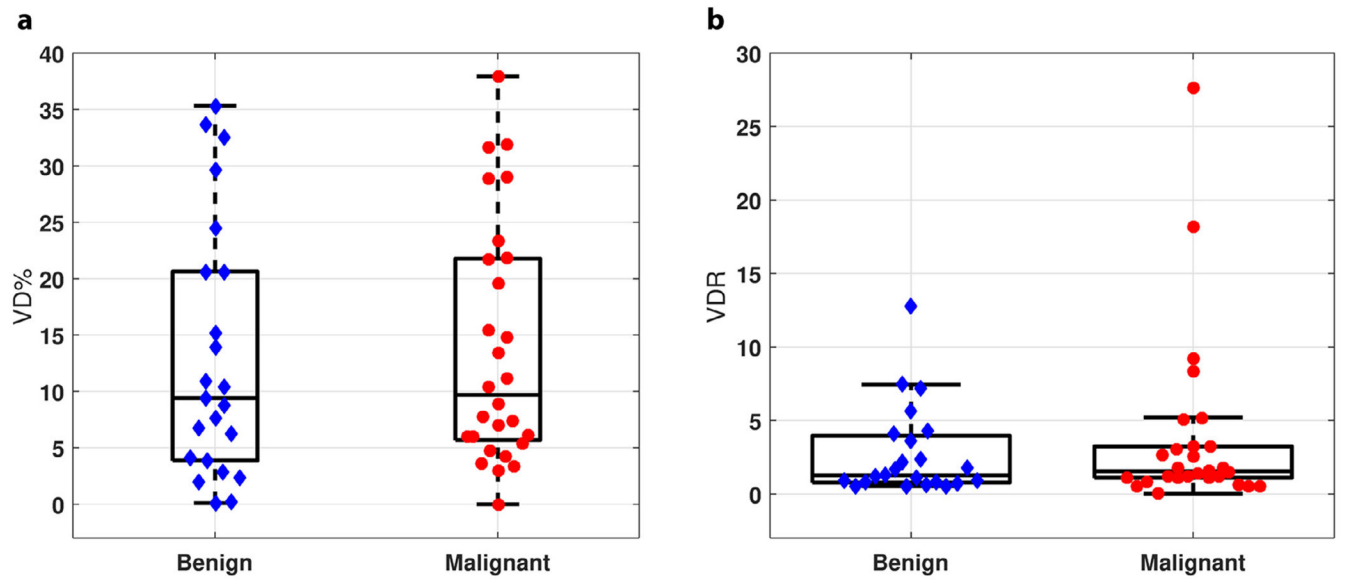
Fig. 3.
Vessel density (VD) and vessel density ratio (VDR) distribution in benign and malignant breast masses by ultrasensitive ultrasound microvessel imaging (UMI). (a) VD distribution in benign and malignant tumors. (b) VDR distribution in benign and malignant tumors.
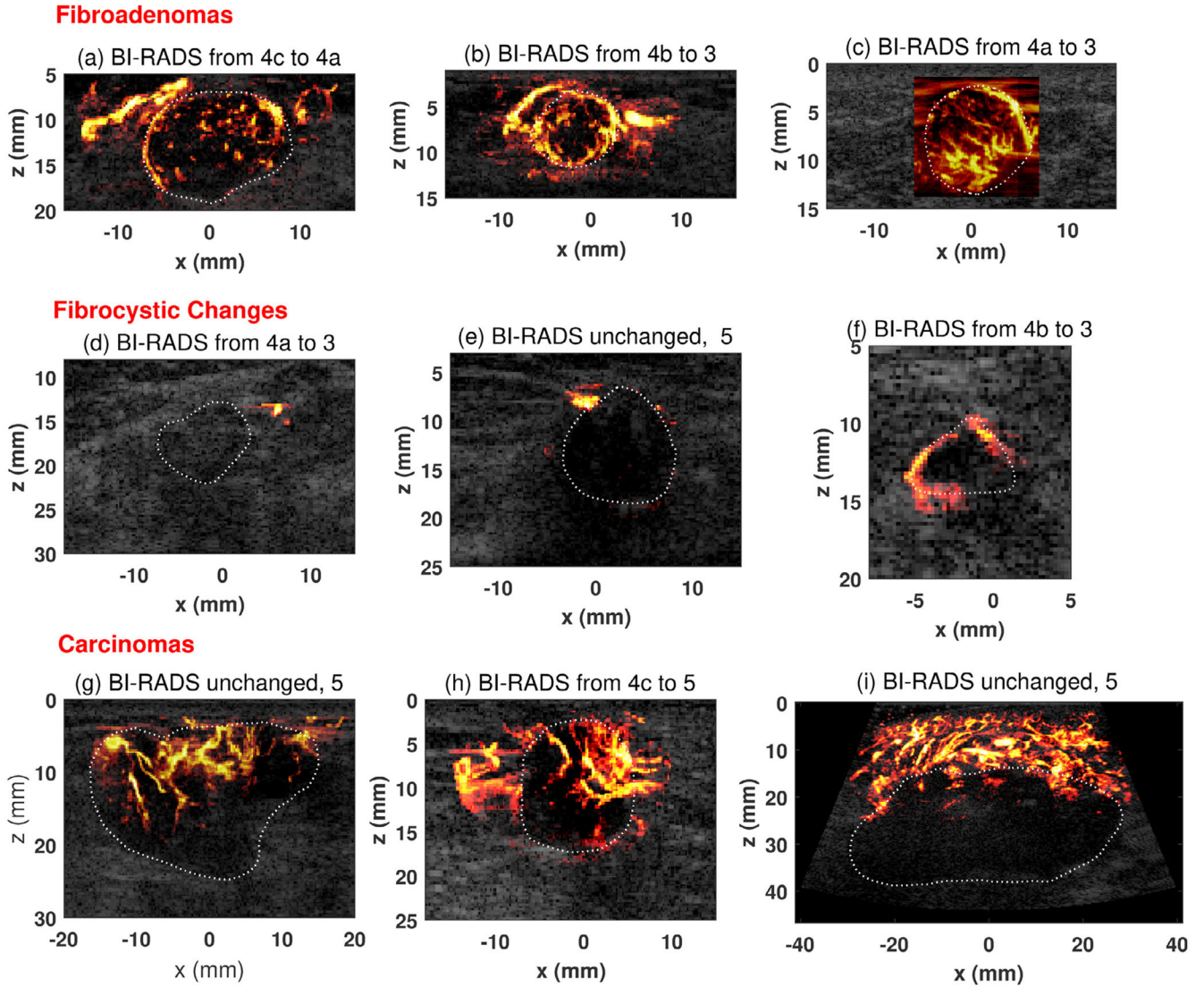
Fig. 4.
Representative ultrasensitive ultrasound microvessel imaging (UMI) of different types of breast masses. (a) Fibroadenoma from a 34-y-old woman. Maximum mass diameter: 2.34 cm. (b) Fibroadenoma from a 34-y-old woman. Maximum mass diameter: 1.3 cm. (c) Fibroadenoma from a 27-y-old woman; Maximum mass diameter: 2.0 cm. (d) A mass of fibrocystic change from a 67-y-old woman. Maximum mass diameter: 2.75 cm. (e) A mass of fibrocystic change from a 74-y-old woman. Maximum mass diameter: 1.3 cm. (f) A mass of fibrocystic change from a 52-y-old woman. Maximum mass diameter: 1.0 cm. (g) Nottingham grade II (of III) invasive lobular carcinoma from a 79-y-old woman. Maximum mass diameter: 3.0 cm. (h) Nottingham grade II (of III) invasive ductal carcinoma from an 83-y-old man. Maximum mass diameter: 1.7 cm. (i) Nottingham grade III (of III) adenocarcinoma (poorly differentiated) from a 43-y-old woman. Maximum mass diameter: 5.0 cm. The mass boundaries were delineated with *white dashed lines* to help readers appreciate the performance of UMI. Note that BI-RADS scoring and adjustment of BI-
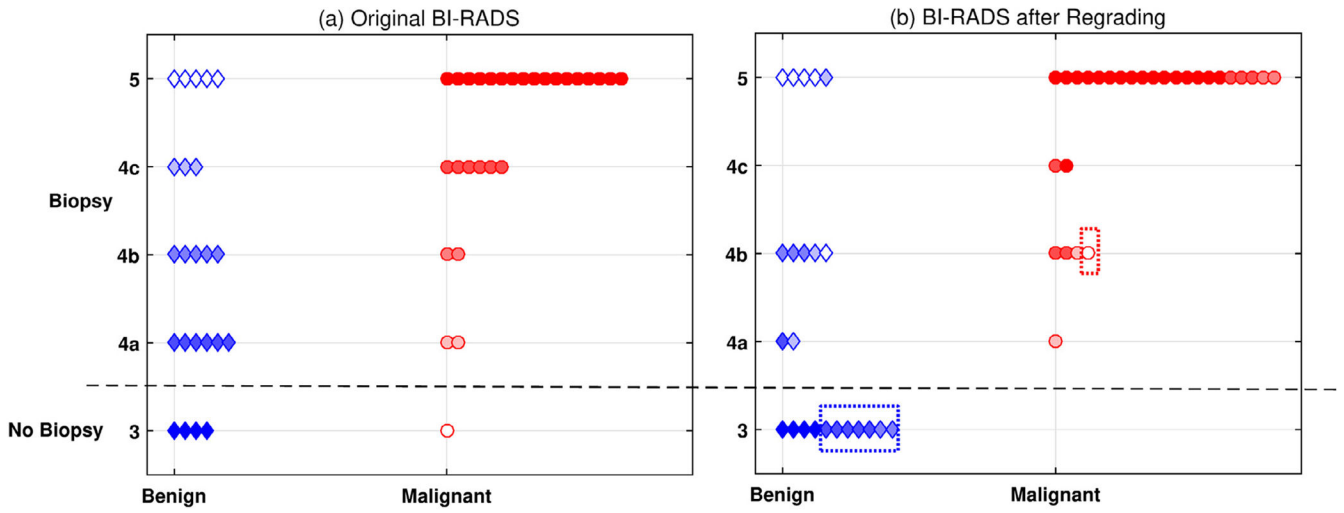
RADS categories using UMI images did not require delineation of tumor boundary. BI-RADS = Breast Imaging Reporting and Data System.

Fig. 5.
Comparison of BI-RADS scores for 51 masses before and after regrading with ultrasensitive ultrasound microvessel imaging. (a) BI-RADS scores for the 51 masses scored by an experienced radiologist, who was blinded to the pathology results, using conventional ultrasonography scan images. Benign and malignant tumors with different BI-RADS categories are coded with different colors. (b) Regraded BI-RADS based on both conventional ultrasound and ultrasensitive ultrasound microvessel imaging by the same radiologist. The *blue dashed box* indicates seven corrected false-positive cases, and the *red dashed box* indicates the corrected false-negative cases. BI-RADS = Breast Imaging Reporting and Data System.

Table 1.

Histopathology results (n = 51)

Benign	23 (45.1%)
Fibroadenoma	15 (29.5%)
Fibrocystic breast changes	6 (11.8%)
Lactating adenoma	1 (1.9%)
Focal pseudoangiomatous stromal hyperplasia (PASH).	1 (1.9%)
Malignant	28 (54.9%)
Invasive ductal carcinoma	18 (35.3%)
Invasive lobular carcinoma	4 (7.9%)
Invasive mammary carcinoma	4 (7.9%)
Ductal carcinoma *in situ*	1 (1.9%)
Adenocarcinoma [*]	1 (1.9%)

[*] Poorly differentiated adenocarcinoma, morphologically consistent with breast primary. No further analysis available.

Table 2.

Criteria for regrading BI-RADS scores based on microvessel morphology in ultrasensitive ultrasound microvessel imaging

Agree well with benign tumors	−2
Partially agree with benign tumors	−1
No obvious benign or malignant features	0
Partially agree with malignant tumors	+1
Agree well with malignant tumors	+2
Benign tumor vessel features	Malignant tumor vessel feature
Regular/linear vessels	Chaotic vessel distribution with irregular branches
Intratumor vessels isolated from peritumor vessels	Intra- and peri-tumor vessels closely connected Penetrating vessels from periphery
Fibroadenoma: continuous vessel flow along the boundary	
Fibrocystic change: Avascular/hypovascular at both center and periphery	

BI-RADS = Breast Imaging Reporting and Data System.

Table 3.

Comparison of classification performance

	Conventional US	Conventional US + UMI
Sensitivity	96.43% 95% CI: 81.65%–99.91% 27/28	100.00% 95% CI: 87.66%–100% 28/28
Specificity	17.39% 95% CI: 4.95%–38.37% 4/23	47.83% CI: 26.82%–69.41% 11/23
Positive predictive value	58.70% 95% CI: 53.76%–63.46% 27/46	70.00% 95% CI: 61.21%–77.53% 28/40
Negative predictive value	80.00% 95% CI: 32.42%–97.09% 4/5	100.00% 11/11
Diagnostic accuracy	60.78% 95% CI: 46.11%–74.16% 31/51	76.47% 95% CI: 62.51%–87.21% 39/51

US = ultrasonography; UMI = ultra-sensitive ultrasound microvessel imaging; CI = confidence interval.